Supporting information

1. Schematic of the stacking process for the fabrication of heterostructures

Monolayers of WS_2 and $MoSe_2$ and few layers of hBN were prepared by mechanical stripping, respectively. To active modulation of the twist angle between the layers of $MoSe_2/WS_2$. The second harmonic generation (SHG) signals of the monolayer WS_2 and $MoSe_2$ need to be tested sequentially before stacking to obtain the corresponding crystal orientations. Afterward, a Polycarbonate (PC) film was bonded to the Polydimethylsiloxane (PDMS) surface and combined with a few layers of hBN as a pick-up "gripper" to pick up $MoSe_2$ first, and based on the second harmonic generation results, the position of $MoSe_2$ and WS_2 was adjusted to the interlayer angle of θ by controlling the deflection angle of the displacement stage with high-precision transfer, then WS_2 was picked up, and hBN was picked up by repeating the above steps, to obtain the hBN/$MoSe_2$/WS_2/hBN heterojunction. The friction vice prepared above was immersed in chloroform for 2 min to remove the residual adhesive film on the surface of the sample to ensure a clean surface. Finally, the samples were stored in a vacuum environment and heated to 280 °C for annealing for 8 hours.

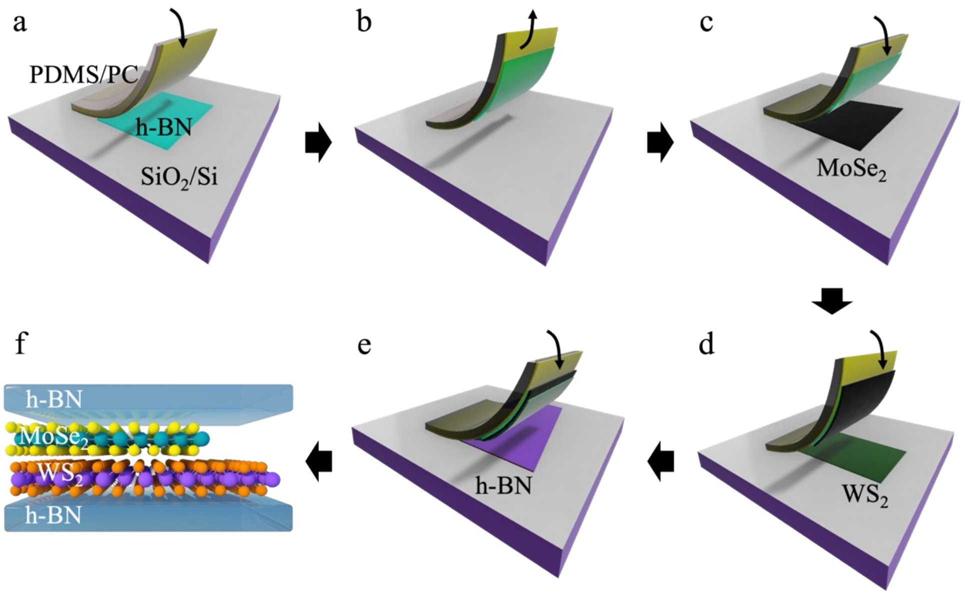

Figure S1 Pick and left technology for assembly of van der Waals heterostructures. (a–f) Sequential device fabrication method, describing the tear-and-stack co-lamination process used to create the hBN/$MoSe_2$/WS_2/hBN/ stacks.

2. Lifetime components filtered by 785/60 nm bandpass filter

To eliminate the effect of the instrumental response function (IRF), we used the tail-fitting method. The fitting results are shown in Table S1. Among them, the short-lived component (τ_1) is attributed to the hybridized exciton. The long-lived component (τ_2) is attributed to effects related to surface defect, substrate and strains.

Table S1. Twist-angle dependent exciton lifetimes and population

twist angle (°)	τ_1 (ns)	A_1 (%)	τ_2 (ns)	A_2 (%)
1	3.32	93.7	0.57	6.3
3	2.73	91.4	0.55	8.6
5	1.38	91.1	0.58	8.9
7	1.13	93.9	0.553	6.1
10	0.54	94.0	0.54	6.0
12	0.502	92.2	0.502	7.8